TU Delft

Delft University of Technology

A Low-Complexity Time Synchronization Algorithm for MIMO ZP-OFDM in Urban Impulsive Noise Environments

Roshandeh, Koosha Pourtahmasi; Mohammadkarimi, Mostafa; Ardakani, Masoud

DOI
10.1109/GLOBECOM54140.2023.10437433

Publication date
2023

Document Version
Final published version

Published in
GLOBECOM 2023 - 2023 IEEE Global Communications Conference

Citation (APA)
Roshandeh, K. P., Mohammadkarimi, M., & Ardakani, M. (2023). A Low-Complexity Time Synchronization Algorithm for MIMO ZP-OFDM in Urban Impulsive Noise Environments. In *GLOBECOM 2023 - 2023 IEEE Global Communications Conference* (pp. 4211-4216). (Proceedings - IEEE Global Communications Conference, GLOBECOM). IEEE. https://doi.org/10.1109/GLOBECOM54140.2023.10437433

Important note
To cite this publication, please use the final published version (if applicable).
Please check the document version above.

Copyright
Other than for strictly personal use, it is not permitted to download, forward or distribute the text or part of it, without the consent of the author(s) and/or copyright holder(s), unless the work is under an open content license such as Creative Commons.

Takedown policy
Please contact us and provide details if you believe this document breaches copyrights.
We will remove access to the work immediately and investigate your claim.

This work is downloaded from Delft University of Technology.
For technical reasons the number of authors shown on this cover page is limited to a maximum of 10.

Green Open Access added to TU Delft Institutional Repository

'You share, we take care!' - Taverne project

https://www.openaccess.nl/en/you-share-we-take-care

Otherwise as indicated in the copyright section: the publisher is the copyright holder of this work and the author uses the Dutch legislation to make this work public.

A Low-Complexity Time Synchronization Algorithm for MIMO ZP-OFDM in Urban Impulsive Noise Environments

Koosha Pourtahmasi Roshandeh*, Mostafa Mohammadkarimi†, and Masoud Ardakani*
*Electrical and Computer Engineering Department, University of Alberta
†Faculty of Electrical Engineering, Mathematics and Computer Science, Delft University of Technology
pourtahm@ualberta.ca, m.mohammadkarimi@tudelft.nl, ardakani@ualberta.ca

GLOBECOM 2023 - 2023 IEEE Global Communications Conference | 979-8-3503-1090-0/23/$31.00 ©2023 IEEE | DOI: 10.1109/GLOBECOM54140.2023.10437433

***Abstract*—The zero padding (ZP) variants of orthogonal frequency-division multiplexing (OFDM) exhibit a lower bit error rate (BER) and higher energy efficiency compared to their cyclic prefix (CP) counterparts. However, the employment of ZP-OFDM demands strict time synchronization, which is challenging in the absence of pilots or CP. Moreover, time synchronization in OFDM systems is even more challenging when impulsive noise is present. It is well known that urban noise, which consists largely of impulsive noise generated by spark plugs used in internal combustion engines, switching and industrial activities, and discharge of high voltage distribution lines, has a strong influence on digital mobile communications. In this paper, we propose a new low-complexity approximate maximum likelihood (A-ML) timing offset (TO) estimator for ZP multiple-input multiple-output (MIMO)-OFDM in impulsive-noise environments. Performance comparison of the A-ML estimator with existing TO estimators demonstrates a superior performance in terms of lock-in probability with similar computational complexity. Also, compared to the optimal ML TO estimator, it offers a significantly lower computational complexity with negligible performance loss. The A-ML estimator can be employed for both frame and symbol synchronization.**

I. Introduction

Orthogonal frequency-division multiplexing (OFDM) [1] is used in many wireless standards, such as, IEEE 802.15.3a, IEEE 802.16d/e, IEEE 802.15.4g, 3GPP-LTE, and LTE-Advanced. In addition, OFDM-based waveforms combined with massive MIMO and/or intelligent reflecting surface are promising new technologies for achieving both spectrum and energy efficient wireless communications. Moreover, many internet of things (IoT) applications, such as smart buildings and vehicle-to-everything (V2X) leverage OFDM as their main communication scheme [2], [3].

OFDM is susceptible to inter symbol interference (ISI) caused by the high selectivity of the fading channel [4]. In order to mitigate this issue, usually a guard interval with a fixed length is inserted between every two consecutive OFDM symbols. When the guard interval is a partial repetition of the transmitting data samples, this scheme is called cyclic prefix (CP)-OFDM [5]. When the guard interval is filled with zeros, the scheme is called zero-padded (ZP)-OFDM [6]. The primary benefit of CP-OFDM over ZP-OFDM is the ease of timing offset (TO) estimation or equivalently estimating the starting point of the received samples to take fast Fourier transform (FFT). This time synchronization is easily carried out by using CP. Despite the ease of time synchronization, CP-OFDM has some major disadvantages such as extra power transmission and a higher BER compared to ZP-OFDM [7]. While ZP-OFDM does not have such drawbacks, its time synchronization or equivalently TO estimation is more complex [8]. There are two approaches for TO estimation of ZP-OFDM. In the first approach, called data-aided (DA) time synchronization, a series of training sequences (pilots) is inserted in the OFDM blocks and are used for TO. The second approach, referred to as non-data-aided (NDA) time synchronization relies on the statistical properties of the transmitted signal and the multipath fading channel. In this paper, we propose a new low-complexity NDA TO estimator for ZP-OFDM in practical impulsive-noise environments.

1) Related work: The DA time synchronization for ZP-OFDM has been studied in [9], where a highly correlated training sequence (pilot) is employed to increase the autocorrelation of the received signal, which is then used for estimating the TO. Such a pilot-based time synchronization algorithm can achieve reliable performance while having a reasonable complexity [9]. For NDA, however, a low-complexity high-accuracy TO estimation algorithm does not exist. Existing NDA time synchronization algorithms for ZP-OFDM [10], [11] are mainly heuristic energy-based algorithms. Such methods generally use a sliding window to detect the starting point of the zero pad. Energy-based techniques greatly suffer from the natural randomness of the received samples; thus, exhibit poor performance in terms of lock-in probability, i.e. correct TO estimation. A mathematical approach towards NDA TO estimation for ZP-OFDM has been proposed in [8], and the optimal maximum likelihood (ML) TO estimator for ZP-OFDM has been derived. The optimal NDA estimator is highly complex which hinders its implementation for MIMO systems.

2) Motivation: ZP-OFDM and its variants, e.g. ZP-OTFS [12], and RP-OTFSM [13], are promising candidates for 6G wireless systems requiring joint communication and sensing [1]. ZP-OFDM based waveforms have several advantages compared to CP-OFDM [14]. For example, regardless of the channel nulls, it is possible to perform finite impulse response equalization in ZP-OFDM systems [7]. Moreover, channel estimation and tracking is easier in ZP-OFDM compared to CP-OFDM [7]. Finally, ZP-OFDM requires less transmission power compared to CP-OFDM, due to lack of CP, which makes it a suitable candidate for power-limited devices.

Authorized licensed use limited to: TU Delft Library. Downloaded on February 10,2025 at 13:06:46 UTC from IEEE Xplore. Restrictions apply.

However, time synchronization becomes challenging in ZP-OFDM, and existing algorithms fail to achieve a high lock-in probability, or practical complexity. Moreover, existing TO estimators for ZP-OFDM so far are developed for Gaussian noise models. However, many real-world channels, e.g. underwater, urban and indoor channels, are known to experience impulsive noise, rather than a simple Gaussian noise [15]. In urban environments, the sources of impulsive noise are mainly the unintelligible traces of switching and industrial activities, corona discharge of high voltage distribution lines, or automotive electronics. Design of communication systems and specifically time synchronization algorithm under simple Gaussian noise model can be significantly suboptimal when impulsive noise is present [16]. Hence, an accurate yet low-complexity time synchronization algorithm for ZP-OFDM in impulsive noise is needed. The goal of this paper is to fill this existing gap. Specifically,

- we derive the approximate probability density function (PDF) of the received ZP-OFDM samples,
- we propose a low-complexity approximate ML (A-ML) TO estimator for MIMO ZP-OFDM systems in highly time-frequency selective channels with impulsive noise. This algorithm,
  - achieves a significantly higher lock-in probability compared to [10] whilst having a negligible perofrmance loss compared to [8]
  - has significantly lower complexity than the ML estimator of [8],
  - is suitable for deployment in very low signal-to-noise ratio (SNR) values in contrast to [8],
- we analyze the complexity of the proposed estimator.

II. System and Signal Model

We consider a MIMO-OFDM wireless system with transmission bandwidth B, and $m_{\rm t}$ and $m_{\rm r}$ transmit and receive antennas, respectively. This system uses ZP-OFDM to communicate over a time-frequency selective Rayleigh fading channel. Let $\{x_m^{(n,k)}\}_{k=0}^{n_{\rm x}-1}$, $\mathbb{E}\{|x_m^{(n,k)}|^2\} = \sigma_{\rm x}^2/m_{\rm t}$ denote the $n_{\rm x}$ number of the complex modulated symbols from the n-th OFDM block to be transmitted from the m-th transmit antenna. The corresponding complex baseband OFDM signal can be expressed as

$$x_m^{(n)}(t) = \sum_{k=0}^{n_{\rm x}-1} x_m^{(n,k)} e^{\frac{j2\pi kt}{T_{\rm x}}}, \qquad 0 \le t \le T_{\rm x}, \tag{1}$$

where $T_{\rm x} = n_{\rm x}/B$ denotes the duration of the payload signal. A zero-padding guard interval of length $T_{\rm z}$ is added to (1). Hence, the n-th transmitted OFDM block from the m-th transmit antenna is given by

$$s_m^{(n)}(t) = \begin{cases} x_m^{(n)}(t) & 0 \le t \le T_{\rm x} \\ 0 & T_{\rm x} < t \le T_{\rm s}, \end{cases} \tag{2}$$

where $T_{\rm s} = T_{\rm x} + T_{\rm z}$ denotes the time duration of a ZP-OFDM block. Let $f_{\rm s} \triangleq 1/T_{\rm sa} = n_{\rm x}/T_{\rm x} = B$, and $\{h_{qm}[k,l]\}_{l=0}^{n_{\rm h}-1}$ denote the sampling rate at the receiver and the $n_{\rm h}$ channel taps between the transmit antenna m and the receive antenna q at time instance k, respectively. The channel taps are assumed to be statistically independent circularly symmetric complex Gaussian (CSCG) random variables, i.e. Rayleigh fading, with the cross-correlation as

$$\begin{aligned} &\mathbb{E}\{h_{q_1m_1}[k_1,l]h^*_{q_2m_2}[k_2,l-u]\} = \\ &\quad \sigma^2_{{\rm h}_l} R[k1-k2]\delta[u]\delta[q_1-q_2]\delta[m_1-m_2] \end{aligned} \tag{3}$$

for $l = 0, 1, \ldots, n_{\rm h}-1$, where $\mathbb{E}\{\cdot\}$, $*$, and $\delta[\cdot]$ denote the statistical, expectation, complex conjugate, and Dirac delta function, respectively. The function $R[k]$ in (3) is an arbitrary function with $R[0] = 1$ and $|R[k]| < 1$. As the relative speed of the transmitter and the receiver increases, $R[k]$ approaches $\delta[k]$. For PDF analysis of the received samples, we consider

$$\begin{aligned} &\mathbb{E}\{h_{q_1m_1}[k_1,l]h^*_{q_2m_2}[k_2,l-u]\} = \\ &\quad \sigma^2_{{\rm h}_l} \delta[k_1-k_2]\delta[u]\delta[q_1-q_2]\delta[m_1-m_2]; \end{aligned} \tag{4}$$

however, the proposed A-ML estimator works for any arbitrary function $R[k]$ with little performance degradation. It is assumed that the power delay profile (PDP) of the fading channel, i.e., $\sigma^2_{{\rm h}_l}$, $l = 0, 1, \ldots, n_{\rm h}-1$, is priori known at the receiver and has already been estimated during channel sounding. In the absence of synchronization error and ISI, the discrete received baseband vector is expressed as

$$\mathbf{y}^{(n)} = \begin{cases} \mathbf{H}\mathbf{s}^{(n)} + \mathbf{w}^{(n)}, & n \ge 0 \\ \mathbf{w}^{(n)}, & n < 0, \end{cases} \tag{5}$$

where $\mathbf{H}$ denotes the discrete channel matrix including the effect of the transmit and received filter, and is defined as

$$\mathbf{H} = \begin{pmatrix} \mathbf{H}_{11} & \mathbf{H}_{12} & \cdots & \mathbf{H}_{1m_{\rm t}} \\ \mathbf{H}_{21} & \mathbf{H}_{22} & \cdots & \mathbf{H}_{2m_{\rm t}} \\ \vdots & \cdots & \ddots & \cdots \\ \mathbf{H}_{m_{\rm r}1} & \mathbf{H}_{m_{\rm r}2} & \cdots & \mathbf{H}_{m_{\rm r}m_{\rm t}}, \end{pmatrix}. \tag{6}$$

In (6), $\mathbf{H}_{qm}$ is the $n_{\rm s} \times n_{\rm s}$ lower triangular channel matrix between the transmit antenna m and the receive antenna q with the $(k+1)$th column as $[\mathbf{0}_k^{\rm T}\ h_{qm}[nn_{\rm s}+k,0]\ h_{qm}[nn_{\rm s}+k,1]\ \ldots\ h_{qm}[nn_{\rm s}+k,n_{\rm h}-1]\ \mathbf{0}_{n_{\rm s}-n_{\rm h}-k}^{\rm T}]^{\rm T}$, $0 \le k \le n_{\rm s}-1$, where $\mathbf{0}_k$ is the all-zero vector of length k. We define $n_{\rm s} = n_{\rm x} + n_{\rm z}$, where $n_{\rm s} \triangleq T_{\rm s}/T_{\rm sa}$ $n_{\rm x} \triangleq T_{\rm x}/T_{\rm sa}$, and $n_{\rm z} \triangleq T_{\rm z}/T_{\rm sa}$ denote the number of OFDM signal samples, the number of data samples, and the number of noise-only samples, respectively. The vectors $\mathbf{s}^{(n)}$, $\mathbf{y}^{(n)}$, and $\mathbf{w}^{(n)}$ are

$$\mathbf{s}^{(n)} = \begin{pmatrix} \mathbf{s}_1^{(n)} \\ \mathbf{s}_2^{(n)} \\ \vdots \\ \mathbf{s}_{m_{\rm t}}^{(n)} \end{pmatrix},\ \mathbf{y}^{(n)} \triangleq \begin{pmatrix} \mathbf{y}_1^{(n)} \\ \mathbf{y}_2^{(n)} \\ \vdots \\ \mathbf{y}_{m_{\rm r}}^{(n)} \end{pmatrix},\ \mathbf{w}^{(n)} \triangleq \begin{pmatrix} \mathbf{w}_1^{(n)} \\ \mathbf{w}_2^{(n)} \\ \vdots \\ \mathbf{w}_{m_{\rm r}}^{(n)} \end{pmatrix}, \tag{7}$$

where $\mathbf{y}_q^{(n)}$, $\mathbf{w}_q^{(n)}$, and $\mathbf{s}_m^{(n)}$ denote the received vector at the q-th receive antenna, the noise vector at the q-th receive antenna,

Authorized licensed use limited to: TU Delft Library. Downloaded on February 10,2025 at 13:06:46 UTC from IEEE Xplore. Restrictions apply.

and the transmitted vector from the m-th transmit antenna, respectively, and are defined as

$$\mathbf{y}_q^{(n)} \triangleq \Big[y_q^{(n)}[0]\ y_q^{(n)}[1]\ \dots\ y_q^{(n)}[n_\mathrm{s}-1]\Big]^\mathrm{T}, \tag{8a}$$

$$\mathbf{w}_q^{(n)} \triangleq \Big[w_q^{(n)}[0]\ w_q^{(n)}[1]\ \dots\ w_q^{(n)}[n_\mathrm{s}-1]\Big]^\mathrm{T}, \tag{8b}$$

$$\mathbf{s}_m^{(n)} \triangleq \Big[s_m^{(n)}[0]\ s_m^{(n)}[1]\ \dots\ s_m^{(n)}[n_\mathrm{s}-1]\Big]^\mathrm{T}, \tag{8c}$$

$$= \Big[x_m^{(n)}(0)\ x_m^{(n)}(T_\mathrm{sa})\ \dots\ x_m^{(n)}((n_\mathrm{x}-1)T_\mathrm{sa})\ \mathbf{0}_{n_z}^\mathrm{T}\Big]^\mathrm{T}.$$

We also consider the Class A impulsive noise model for $\mathbf{w}_q^{(n)}$, i.e. Gaussian mixtures, that its PDF is defined as [15]

$$f_{W_q^{(n)}[k]}(w) = \sum_{l=0}^{L-1} p_l \mathcal{CN}(w:0,\sigma_{\mathrm{w}_l}^2), \tag{9}$$

for $k \in \{0,1,\cdots,n_\mathrm{s}-1\}$, and $\sum_{l=0}^{L-1} p_l = 1$. The Gaussian mixture noise is a more accurate noise model than the conventional Gaussian model in many real-world channels

Based on the Central Limit Theorem, the OFDM samples, i.e. $s_m^{(n)}[k] = x_m^{(n)}(kT_\mathrm{sa}),\ \forall k \in \{0,1,\cdots,n_\mathrm{x}-1\}$, can be modeled as independent and identically distributed (i.i.d) zero-mean CSCG random variables as

$$s_m^{(n)}[k] \text{ or } x_m^{(n)}(kT_\mathrm{sa}) \sim \mathcal{CN}\Big(0,\frac{\sigma_\mathrm{x}^2}{m_\mathrm{t}}\Big), \tag{10}$$

where

$$\mathbb{E}\Big\{s_m^{(n)}[k]s_p^{(n)}[k']^*\Big\} = \mathbb{E}\Big\{x_m^{(n)}(kT_\mathrm{sa})x_p^{(n)}(k'T_\mathrm{sa})^*\Big\} \tag{11}$$

$$= \frac{\sigma_\mathrm{x}^2}{m_\mathrm{t}}\delta[k-k']\delta[m-p], \quad n \in \{0,\mathbb{N}\},$$

for $m,p \in \{1,2,\cdots,m_\mathrm{t}\}$ and $k,k' \in \{0,1,\cdots,n_\mathrm{x}-1\}$.

Now, assume that there is a TO $\tau \triangleq dT_\mathrm{sa} + \epsilon$ between the transmitter and the receiver, where d and ϵ represent the integer and fractional part of the TO, respectively. Since the fractional part of TO, ϵ, can be corrected through channel equalization and carrier frequency offset estimation [17], it suffices to estimate the beginning of the received OFDM vector within one sampling period. Hence, we focus on estimating the integer part of the TO, d.

III. Approximate ML TO Estimator

In this section, we propose the A-ML estimator for estimating d. For the simplicity of the derivation, we first consider the single-input single-output (SISO) scenario. The extension to MIMO systems is straightforward and is briefly discussed.

For $m_\mathrm{t} = m_\mathrm{r} = 1$, we remove the subscripts m and q to simplify the notations. Thus, (5) can be rewritten as

$$\mathbf{y}^{(n)} = \begin{cases} \mathbf{H}\mathbf{s}^{(n)} + \mathbf{w}^{(n)} \triangleq \mathbf{v}^{(n)} + \mathbf{w}^{(n)}, & n \geq 0 \\ \mathbf{w}^{(n)}, & n < 0 \end{cases}, \tag{12}$$

where $\mathbf{H} = \mathbf{H}_{11}$, $\mathbf{v}_m^{(n)} \triangleq \big[v^{(n)}[0]\ v^{(n)}[1]\ \dots\ v^{(n)}[n_\mathrm{s}-1]\big]^\mathrm{T}$. We allow the integer part of the TO, d, take values from the set $\mathcal{D} = \{-n_\mathrm{s}+1,\cdots,-1,0,1,\cdots,n_\mathrm{s}-1\}$. Note that the negative values of the TO, d, corresponds to situations when the receiver starts early to receive samples. That is, for $d<0$, the receiver receives $|d|$ noise samples, and then receives the transmitted OFDM samples starting from the $(|d|+1)$-th sample at the receiver. Similarly, when $d \geq 0$, the receiver starts late to receive the samples. In other words, the receiver misses the first d samples from the transmitted OFDM samples. Allowing d to take both negative and positive values enables the A-ML estimator to perform both frame and symbol synchronization.

The problem of estimating the TO can be formulated as a multiple hypothesis testing problem. Let H_d denote the hypothesis corresponding to when the TO value is $d \in \mathcal{D} = \{-n_\mathrm{s}+1,\cdots,n_\mathrm{s}-1\}$. We first assume that the receiver uses N observation vectors, $\mathbf{y}^{(0)}$, $\mathbf{y}^{(1)}$, $\cdots$, $\mathbf{y}^{(N-1)}$, each with length n_s, in order to estimate the TO d. Later, we allow the receiver to use any arbitrary number of received samples for estimation, not necessarily a multiple of n_s. In order to derive the ML TO estimator, we need to obtain the joint PDF of the N observation vectors under the different hypotheses H_d, $d \in \mathcal{D}$, i.e., $f(\mathbf{y}^{(0)},\mathbf{y}^{(1)},\cdots,\mathbf{y}^{(N-1)}|H_d)$. Lemma 1 from [8] gives some insights about the observation samples.

Lemma 1. *For a Rayleigh fading channel with the cross-correlation function in* (4)*, the observation samples $y^{(n)}[k]$ given H_d are uncorrelated random variables for any arbitrary $n \in \{0,\mathbb{N}\}$ and $0 \leq k \leq n_\mathrm{s}-1$. Moreover, $y^{(n_1)}[k_1]$ and $y^{(n_2)}[k_2]$ are independent random variables for $|(n_1-n_2)n_\mathrm{s}+(k_1-k_2)| > n_\mathrm{h}$, $n_1,n_2 \in \{0,\mathbb{N}\}$ and $0 \leq k_1,k_2 \leq n_\mathrm{s}-1$.*

According to Lemma 1, although the elements of the observation vectors, i.e $y^{(n)}[k]$, are uncorrelated, and those with time index difference greater than n_h are independent, but, they are not generally independent. The possible dependence for the observation samples with time index difference less than n_h makes deriving a closed-form expression for the joint PDF, i.e. $f(\mathbf{y}^{(0)},\mathbf{y}^{(1)},\cdots,\mathbf{y}^{(N-1)}|H_d)$, challenging. However, since a large number of received samples, both from each observation vector and from different observation vectors are independent, we continue by assuming that the received samples are independent. This allows us to find the joint PDF of the received samples under a mild independence assumption

$$f(\mathbf{y}^{(0)},\cdots,\mathbf{y}^{(N-1)}|H_d) \approx \prod_{n=0}^{N-1}\prod_{k=0}^{n_\mathrm{s}-1} f_{Y^{(n)}[k]}(y^{(n)}[k]|H_d), \tag{13}$$

where from (12), we define random variables, $Y^{(n)}[k]$, $V^{(n)}[k]$, and $W^{(n)}[k]$ as $Y^{(n)}[k] = V^{(n)}[k] + W^{(n)}[k]$. Here, the capital letters are used to denote random variables. In [8], the authors have derived closed-form expressions for the exact PDF of $V^{(n)}[k]$ and $Y^{(n)}[k]$ for $n \in \mathbb{Z}$ and $0 \leq k \leq n_\mathrm{s}-1$. The histogram density estimation and statistical higher-order moment analyses, such as the kurtosis and skewness analysis, show that the distribution of the random variable $V^{(n)}[k] = V[nn_\mathrm{s}+k]$ given hypothesis H_0 can be accurately

Authorized licensed use limited to: TU Delft Library. Downloaded on February 10,2025 at 13:06:46 UTC from IEEE Xplore. Restrictions apply.

approximated by a CSCG PDF as

$$V^{(n)}[k]|H_0 = V[nn_{\rm s}+k]|H_0 \sim \mathcal{CN}(0,\sigma_k^2), \tag{14}$$

where σ_k^2 is the variance of the exact distribution in [8] as

$$\sigma_k^2 \triangleq \mathbb{E}\{\left|V^{(n)}[k]\right|^2|H_0\} \tag{15}$$
$$= \begin{cases} \sum_{u=a}^{b}\sigma_{h_u}^2\sigma_{\rm x}^2 & 0\le k<n_{\rm x}+n_{\rm h}-2 \\ & \text{when } n\ge 0 \\ 0 & n_{\rm x}+n_{\rm h}-1\le k\le n_{\rm s}-1 \\ & \text{or } n<0 \end{cases}$$

with

$$(a,b)=\begin{cases}(0,k) & 0\le k\le n_{\rm h}-2\\ (0,n_{\rm h}-1) & n_{\rm h}-1\le k\le n_{\rm x}-1\\ (k-n_{\rm x}+1,n_{\rm h}-1) & n_{\rm x}\le k\le n_{\rm x}+n_{\rm h}-2.\end{cases} \tag{16}$$

Fig. 1 compares the empirical PDF of the in-phase component of received samples $k=1$ and $k=150$ with the Gaussian PDF approximation with variance $\sigma_k^2/2$. Moreover, Table I, compares the empirical kutosis and skewness of the received samples $k=1$ and $k=150$ with the Gaussian PDF approximation. As seen, the Gaussian PDF in (14) can accurately approximate the exact PDF. Using Equations (15) and (16), we define the vector of variances associated with the received samples given hypothesis H_0 as $\boldsymbol{\sigma}^2_{\mathbf{V}|H_0} \triangleq$

$$\begin{bmatrix}\vdots\\ \sigma^2_{\mathbf{V}[-2]|H_0}\\ \sigma^2_{\mathbf{V}[-1]|H_0}\\ \hdashline \sigma^2_{\mathbf{V}[0]|H_0}\\ \sigma^2_{\mathbf{V}[1]|H_0}\\ \vdots\\ \sigma^2_{\mathbf{V}[n_{\rm s}-1]|H_0}\\ \hdashline \sigma^2_{\mathbf{V}[n_{\rm s}]|H_0}\\ \sigma^2_{\mathbf{V}[n_{\rm s}+1]|H_0}\\ \vdots\\ \sigma^2_{\mathbf{V}[2n_{\rm s}-1]|H_0}\\ \hdashline \vdots\end{bmatrix} \overset{(a)}{=} \begin{bmatrix}\vdots\\ 0\\ 0\\ \hdashline \sigma_0^2\\ \sigma_1^2\\ \vdots\\ \sigma^2_{n_{\rm s}-1}\\ \hdashline \sigma_0^2\\ \sigma_1^2\\ \vdots\\ \sigma^2_{n_{\rm s}-1}\\ \hdashline \vdots\end{bmatrix} \tag{17}$$

where σ_k^2 is given in (15). The vector of variances given hypothesis H_d, i.e., $\sigma^2_{\mathbf{V}|H_d}$, is the shifted version of $\sigma^2_{\mathbf{V}|H_0}$. Thus, we can write

$$V^{(n)}[k]|H_d = V[nn_{\rm s}+k]|H_d \tag{18}$$
$$\sim \mathcal{CN}\Big(0,\sigma^2_{(nn_{\rm s}+k+d,n_{\rm s})_{\rm r}}\mathbb{I}\{nn_{\rm s}+k+d\}\Big),$$

where $0\le (nn_{\rm s}+k+d,n_{\rm s})_{\rm r}\le n_{\rm s}-1$ denotes the reminder of the division $(nn_{\rm s}+k+d)/n_{\rm s}$, $d\in\mathcal{D}=\{-n_{\rm s}+1,\cdots,-1,0,1,\cdots,n_{\rm s}-1\}$, and

$$I\{x\}=\begin{cases}1 & \text{if } x\ge 0\\ 0 & \text{if } x<0\end{cases} \tag{19}$$

is the indicator function. It should be noted that for $(nn_{\rm s}+k+d)<0$, $\mathcal{CN}(0,0)$ denotes the Dirac delta function. Since $V^{(n)}[k]$ and $W^{(n)}[k]$ are independent random variables, the PDF of $Y[nn_{\rm s}+k]\triangleq Y^{(n)}[k]$ given hypothesis H_d is obtained through the convolution of the PDF of $V[nn_{\rm s}+k]=V^{(n)}[k]$ and the PDF $W[nn_{\rm s}+k]=W^{(n)}[k]$ as

$$f_{Y[k']}(y|H_d)=\sum_{l=0}^{L-1}\frac{p_l}{2\pi\sigma^2_{{\rm w}_l}}\frac{1}{2\pi\sigma^2_{(k'+d,n_{\rm s})_{\rm r}}\mathbb{I}\{k'+d\}}\times$$
$$\int_{-\infty}^{\infty}\exp\left\{\frac{-1}{2\sigma^2_{{\rm w}_l}}\left|y-v\right|^2\right\}\exp\Big(\frac{-|v|^2}{2\sigma^2_{(k'+d,n_{\rm s})_{\rm r}}\mathbb{I}\{k'+d\}}\Big){\rm d}v$$
$$=\sum_{l=0}^{L-1}\frac{p_l}{2\pi(\sigma^2_{{\rm w}_l}+\sigma^2_{(k'+d,n_{\rm s})_{\rm r}}\mathbb{I}\{k'+d\})}\times$$
$$\exp\Big(-\frac{|v|^2}{2(\sigma^2_{{\rm w}_l}+\sigma^2_{(k'+d,n_{\rm s})_{\rm r}}\mathbb{I}\{k'+d\})}\Big), \tag{20}$$

where $k'=nn_{\rm s}+k$. Thus, we can write

$$f_{Y[nn_{\rm s}+k]}(y|H_d)=f_{Y^{(n)}[k]}(y|H_d) \tag{21}$$
$$=\sum_{l=0}^{L-1}p_l\mathcal{CN}\Big(y;0,\sigma^2_{{\rm w}_l}+\sigma^2_{(nn_{\rm s}+k+d,n_{\rm s})_{\rm r}}\mathbb{I}\{nn_{\rm s}+k+d\}\Big).$$

For $K\ge 1$ received samples $\mathbf{y}\triangleq[y[0]\ y[1]\ \cdots\ y[K-1]]^{\rm T}$, by using (13) and (21), we obtain the AL-ML TO as

$$\hat{d}=\underset{d\in\mathcal{D}}{\rm argmax}\prod_{k'=0}^{K-1}f_{Y[k']}(y[k']|H_d)$$
$$=\underset{d\in\mathcal{D}}{\rm argmax}\prod_{k'=0}^{K-1}\sum_{l=0}^{L-1}p_l\mathcal{CN}\Big(y[k';0,\sigma^2_{{\rm w}_l}+\sigma^2_{(k'+d,n_{\rm s})_{\rm r}}\mathbb{I}\{k'+d\}\Big),$$

where $d\in\mathcal{D}=\{-n_{\rm s}+1,\cdots,-1,0,1,\cdots,n_{\rm s}-1\}$.

IV. Extension to MIMO

For MIMO ZP-OFDM, we can write

$$\mathbf{y}_q^{(n)}=\sum_{m=1}^{m_{\rm t}}\mathbf{H}_{qm}\mathbf{s}_m^{(n)}+\mathbf{w}_q^{(n)},\ \forall q\in\{1,2,\cdots,m_{\rm r}\}. \tag{22}$$

Because the elements of the channel matrices $\mathbf{H}_{qm}$ and $\mathbf{H}_{q'm}$ are independent random variables for $q\neq q'$, we can show that $\mathbf{y}_q^{(n)}$ and $\mathbf{y}_{q'}^{(n)}$ are uncorrelated random vectors. The derivation of the exact joint PDF $f\big(\mathbf{y}_1^{(n)},\mathbf{y}_2^{(n)},\ldots,\mathbf{y}_{m_{\rm t}}^{(n)}|H_d\big)$

Authorized licensed use limited to: TU Delft Library. Downloaded on February 10,2025 at 13:06:46 UTC from IEEE Xplore. Restrictions apply.

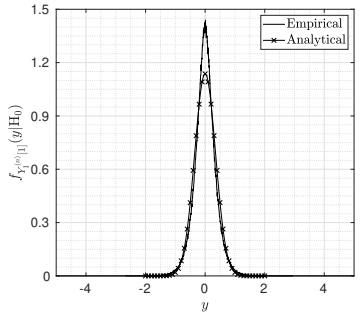

(a)

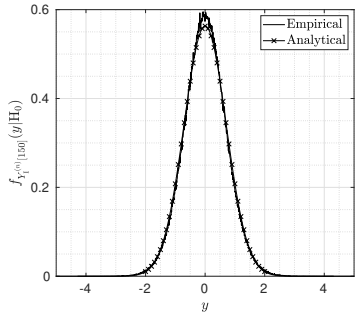

(b)

Fig. 1: The comparison between the empirical PDF of the in-phase component of the received samples and the Gaussian approximation with variance $\sigma_k^2/2$ in (15) for $k = 1$ and $k = 150$.

is not straightforward. However, our statistical analysis shows that $f\big(\mathbf{y}_q^{(n)}|\mathbf{y}_{q'}^{(n)}; H_d\big) \approx f\big(\mathbf{y}_q^{(n)}|H_d\big)$; hence, we can write

$$f\big(\mathbf{y}_1^{(n)}, \mathbf{y}_2^{(n)}, \ldots, \mathbf{y}_{m_\mathrm{t}}^{(n)}|H_d\big) \approx \prod_{q=1}^{m_\mathrm{r}} \prod_{k=0}^{n_\mathrm{s}-1} f_{Y_q^{(n)}[k]}(y_q^{(n)}[k]|H_d). \tag{23}$$

Moreover, similar to the case of SISO, we can show that

$$f_{Y_q[nn_\mathrm{s}+k]}(y|H_d) = f_{Y_q^{(n)}[k]}(y|H_d) \tag{24}$$
$$= \sum_{l=0}^{L-1} p_l \mathcal{CN}\Big(y; 0, \sigma_{\mathrm{w}_l}^2 + \sigma_{(nn_\mathrm{s}+k+d,n_\mathrm{s})_\mathrm{r}}^2 \mathbb{I}\{nn_\mathrm{s}+k+d\}\Big).$$

For $K \geq 1$ received vectors $\mathbf{Y} \triangleq [\mathbf{y}_1\ \mathbf{y}_2\ \ldots \mathbf{y}_q]$, $\mathbf{y}_q \triangleq [y_q[0]\ y_q[1]\ \cdots\ y_q[K-1]]^\mathrm{T}$, by using the independence approximation in (23) and (24) for $k' = nn_\mathrm{s} + k$, we obtain the AL-ML TO as

$$\hat{d} = \underset{d\in\mathcal{D}}{\operatorname{argmax}} \prod_{q=1}^{m_\mathrm{r}} \prod_{k'=0}^{K-1} \sum_{l=0}^{L-1} p_l \times \tag{25}$$
$$\mathcal{CN}\Big(y_q[k']; 0, \sigma_{\mathrm{w}_l}^2 + \sigma_{(k'+d,n_\mathrm{s})_\mathrm{r}}^2 \mathbb{I}\{k'+d\}\Big).$$

Complexity Analysis: The complexity order of the AL-ML, the O-ML [8], the TM [10] estimators, are $\mathcal{O}(m_\mathrm{r} N n_\mathrm{s}|\mathcal{D}|)$, $\mathcal{O}(m_\mathrm{r} M N n_\mathrm{s}|\mathcal{D}|)$, and $\mathcal{O}(m_\mathrm{r} N n_\mathrm{s}|\mathcal{D}|)$, respectively, where M denotes the Monte Carlo samples used for integration in the O-ML estimator [8].

TABLE I: Statistical analysis of the received samples.

	$k=1$		$k=150$	
	Empirical	Analytical	Empirical	Analytical
Mean	-0.00022	0	0.00041	0
Variance	0.1231	0.1232	0.5021	0.5023
Skewness	-0.0048	0	0.0090	0
Kurtosis	4.4519	3	3.3000	3

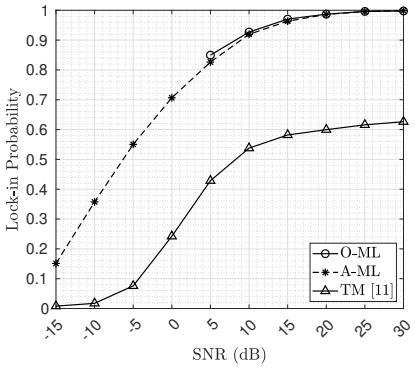

Fig. 2: Performance comparison of the A-ML estimator.

V. Simulations

A ZP-OFDM system with 128-QAM modulation, $B =$ 1MHz, $n_\mathrm{x} = 512$, and $n_\mathrm{z} = 20$ in a frequency-selective Rayleigh fading channel with $n_\mathrm{h} = 10$ channel taps is considered. The exponential channel PDP parameters are $\alpha = 1$ and $\beta = 0.05$, where $\sigma_{\mathrm{h}_l}^2 = \alpha \exp\big(-\beta l\big)$ [8], and the Jakes model with the maximum Doppler shift of $f_\mathrm{D} = 5$ Hz is considered. The number of received OFDM blocks is $N = 10$, and the sampling rate is $f_\mathrm{s} = 10^6$ sample/s. A two-components impulsive noise with parameters $p_0 = 0.99$, $p_1 = 0.01$, $\sigma_{\mathrm{w}_0}^2 = 1$, and $\sigma_{\mathrm{w}_1}^2 = 100$ is considered. The SNR in dB is defined as $\gamma \triangleq 10\log(\sigma_\mathrm{x}^2/\sigma_\mathrm{w}^2)$, $\sigma_\mathrm{w}^2 = p_0\sigma_{\mathrm{w}_0}^2 + p_1\sigma_{\mathrm{w}_1}^2$.

The lock-in probability of the A-ML, the O-ML [8], and the transition metric (TM) [10] TO estimators for different values of E_b/N_0 when $m_\mathrm{t} = m_\mathrm{r} = 1$, $p_0 = 1$, and $p_1 = 0$ are depicted in Fig. 2. As seen, there is a negligible performance gap between the A-ML and the O-ML, whereas the A-ML has a much lower computational complexity. Also, while having the same computational complexity, the A-ML significantly outperforms the TM estimator. Moreover, while the O-ML estimator shows high floating point errors at low E_b/N_0 leading to performance degradation, the A-ML estimator performs relatively well for lower than 5 dB E_b/N_0.

The performance of the proposed A-ML estimator versus the number of observation blocks used for estimation is shown in Fig. 3. As expected, the larger the number of observation blocks, the higher the lock-in probability. Fig. 3 also shows that with a reasonable amount of buffer capacity or an increase in the number of receive antennas, the A-ML is able to achieve high lock-in probability, e.g. more than 0.9 at -10 dB. One can choose the number of observation blocks in A-ML based on the required accuracy and system configuration. The effect of the impulsive noise parameter p_0/p_1 for $\sigma_{\mathrm{w}_0}^2 = 1$ and $\sigma_{\mathrm{w}_1}^2 =$

Authorized licensed use limited to: TU Delft Library. Downloaded on February 10,2025 at 13:06:46 UTC from IEEE Xplore. Restrictions apply.

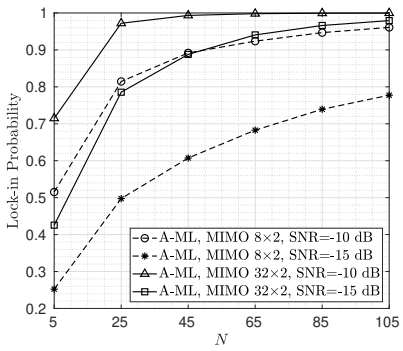

Fig. 3: Lock-in probability versus the number of observation blocks.

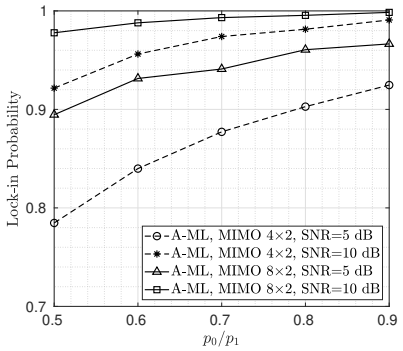

Fig. 4: Lock-in probability for different values of p_0/p_1.

100 on the performance of the A-ML estimator is shown in Fig. 4. As seen, when a component, i.e. $\sigma^2_{\mathrm{w}_0} = 1$, becomes strong, i.e. p_0 increases, the performance improves. This is because the uncertainty of the A-ML estimator arising from Eq. (20) decreases as p_0 increases. Moreover, Fig. 4 shows that the effect of SNR on the lock-in probability is more than the effect of the number of received antennas.

In Fig. 5, the computational complexity of the A-ML estimator is compared with the O-ML estimator in [8] with $M = 10^4$. Here, $t_{\mathrm{A-ML}}$ and $t_{\mathrm{O-ML}}$ denote the average amount of time it takes for the respective algorithms to estimate the TO. As seen, the asymptotic ratio of the completion times is around M for large n_{x} which confirms our analysis.

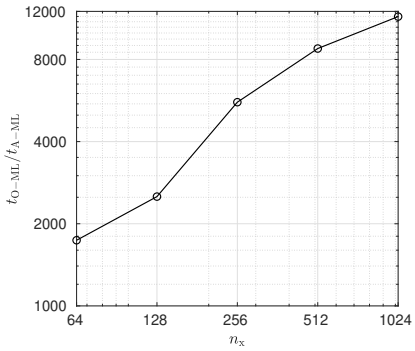

Fig. 5: The ratio of the completion times for different values of n_{x}.

VI. Conclusion

In this paper, we proposed an approximate yet accurate low-complexity NDA ML TO estimator, i.e. A-ML, for MIMO ZP-OFDM systems in highly time-frequency selective fading channels. We showed that the A-ML has orders of magnitude lower complexity than the optimal estimator in [8], i.e. the O-ML, while losing negligible performance in terms of lock-in probability. This makes the A-ML estimator, unlike the O-ML, suitable for practical implementations.

References

[1] S. H. Dokhanchi, A. N. Barreto, and G. Fettweis, "A half-duplex joint communications and sensing system using ZP-OFDM," in *Proc. JC&S*. IEEE, 2022, pp. 1–6.

[2] B. Farhang-Boroujeny and H. Moradi, "OFDM inspired waveforms for 5G," *IEEE Commun. Surveys Tuts.*, vol. 18, no. 4, pp. 2474–2492, 2016.

[3] S. K. Das, F. Benkhelifa, Y. Sun, H. Abumarshoud, Q. H. Abbasi, M. A. Imran, and L. Mohjazi, "Comprehensive review on ML-basedRIS-enhanced IoT systems: Basics, research progress and future challenges," *Computer Networks*, p. 109581, 2023.

[4] X. Wang, P. Ho, and Y. Wu, "Robust channel estimation and ISI cancellation for OFDM systems with suppressed features," *IEEE J. Sel. Areas Commun.*, vol. 23, no. 5, pp. 963–972, May 2005.

[5] S. Roy and C. Li, "A subspace blind channel estimation method for OFDM systems without cyclic prefix," *IEEE Trans. Wireless Commun.*, vol. 1, no. 4, pp. 572–579, Oct. 2002.

[6] B. Muquet, M. de Courville, G. B. Giannakis, Z. Wang, and P. Duhamel, "Reduced complexity equalizers for zero-padded OFDM transmissions," in *Proc. IEEE ICASSP*, Istanbul, Turkey, 2000, pp. 2973–2976.

[7] B. Muquet, Z. Wang, G. B. Giannakis, M. de Courville, and P. Duhamel, "Cyclic prefixing or zero padding for wireless multicarrier transmissions?" *IEEE Trans. Commun.*, vol. 50, no. 12, pp. 2136–2148, 2002.

[8] K. P. Roshandeh, M. Mohammadkarimi, and M. Ardakani, "Maximum likelihood time synchronization for zero-padded OFDM," *IEEE Trans. Signal Process*, vol. 69, pp. 641–654, 2021.

[9] A. A. Nasir, S. Durrani, H. Mehrpouyan, S. D. Blostein, and R. A. Kennedy, "Timing and carrier synchronization in wireless communication systems: a survey and classification of research in the last 5 years," *Eurasip J. Wirel. Commun. Netw.*, no. 1, p. 180, Dec. 2016.

[10] V. Le Nir, T. van Waterschoot, J. Duplicy, and M. Moonen, "Blind coarse timing offset estimation for CP-OFDM and ZP-OFDM transmission over frequency selective channels," *Eurasip J. Wirel. Commun. Netw.*, vol. 2009, no. 1, p. 262813, Jan. 2010.

[11] H. Bolcskei, "Blind estimation of symbol timing and carrier frequency offset in wireless OFDM systems," *IEEE Trans. Commun.*, vol. 49, no. 6, pp. 988–999, Jun. 2001.

[12] S. G. Neelam and P. Sahu, "Digital compensation of IQ imbalance, DC offset for zero-padded OTFS systems," *IEEE Commun. Lett.*, vol. 26, no. 10, pp. 2450–2454, 2022.

[13] P. Karpovich and T. P. Zielinski, "Random-padded OTFS modulation for joint communication and radar/sensing systems," in *Proc. IRS*. IEEE, 2022, pp. 104–109.

[14] G. Kim and D. Yoon, "Analysis of error rate and capacity in the presence of I/Q imbalances over an impulsive noise channel," *IEEE Transactions on Aerospace and Electronic Systems*, 2022.

[15] B. Selim, M. S. Alam, J. V. Evangelista, G. Kaddoum, and B. L. Agba, "NOMA-based iot networks: Impulsive noise effects and mitigation," *IEEE Commun. Mag.*, vol. 58, no. 11, pp. 69–75, 2020.

[16] X. Wang and H. V. Poor, "Robust multiuser detection in non-Gaussian channels," *IEEE Trans. Signal Process.*, vol. 47, no. 2, pp. 289–305.

[17] M. Morelli, C.-C. J. Kuo, and M.-O. Pun, "Synchronization techniques for orthogonal frequency division multiple access (OFDMA): A tutorial review," *Proc. IEEE*, vol. 95, no. 7, pp. 1394–1427, Jul. 2007.

Authorized licensed use limited to: TU Delft Library. Downloaded on February 10,2025 at 13:06:46 UTC from IEEE Xplore. Restrictions apply.